sciendo

DOI 10.2478/ama-2020-0018

acta mechanica et automatica, vol.14 no.3 (2020)

STRESS ASSESSMENT OF GEAR TEETH IN EPICYCLIC GEAR TRAIN FOR RADIAL SEDIMENTATION TANK

Grzegorz BUDZIK,* Tadeusz MARKOWSKI,* Michał BATSCH,* Jadwiga PISULA,* Jacek PACANA,* Bogdan KOZIK*

*Faculty of Mechanical Engineering and Aeronautics, Department of Mechanical Engineering, Rzeszow University of Technology
35-959 Rzeszow, Al. Powstańców Warszawy 8, Poland

gbudzik@prz.edu.pl, tmarkow@prz.edu.pl, mbatsch@prz.edu.pl, jpisula@prz.edu.pl, pacanaj@prz.edu.pl, bogkozik@prz.edu.pl

Received 21 January 2020, revised 18 August 2020, accepted 21 August 2020

Abstract: The paper presents the strength evaluation of planetary gear teeth designed for a radial sedimentation tank drive. A novel type of gear drive, composed of a closed epicyclic gear train and an open gear train with internal cycloidal gear mesh is proposed. Contact stress and root stress in the planetary gear train were determined by the finite element method and according to ISO 6336. The influence of the mesh load factor at planet gears on stress values was also established. A comparison of the results followed. It was observed that the mesh load factor on satellites depends mainly on the way the satellites and central wheels are mounted, the positioning accuracy in the carrier and the accuracy of teeth. Subsequently, a material was selected for the particular design of planetary gear and the assumed load. The analysis of the obtained results allowed assuming that in case of gears in class 7 and the rigid mounting of satellites and central wheels, gears should be made of steel for carburizing and hardening. In case of flexible satellites or flexible couplings in the central wheels and gears in class 4, gears can be made of nitriding steel.

Key words: Planetary gear, FEM, ISO 6336

1. INTRODUCTION

Planetary (epicyclic) gears are gear systems in which at least one gear, called a planet, has no fixed axis, and is instead supported by a rotating part called a carrier. Usually several planet gears are used, so that the transmitted power is distributed, allowing the dimensions of the entire gear system to be reduced. A key factor here is the uniformity of load transfer expressed by the mesh load factor K_γ. Its value determines the percentage share in transmitting power of planet gear. This, as it was proved by Singh (2005, 2010), Ligata et al. (2008), Fernandez del Rincon et al. (2013), Cooley and Parker (2014),Tsai et al. (2015, 2018), by Iglesias et al. (2017), Marques et al. (2016, 2017), and specified in ANSI/AGMA 6123-C16 (2016) standard depends, in particular, on the errors in the fabrication of gears, errors in the positioning on the carrier and the mounting structure of the planets.

The analyzed planetary gear is a part of the drive of a radial sedimentation tank (Fig. 1).

Propulsion is provided by a three-phase squirrel-cage motor, which drives a planetary gear train—the first reduction stage. An electronic control system for the motor should offer a soft start functionality so as to avoid overloading the mechanism. The gear train's output shaft connects to a pinion (a), which engages with an internal gear (b). The gear (b) is attached to a scraper (c), which is bearing-supported on the axis (d) of a sedimentation tank (e). In the present solution, the gear train in the second reduction stage (gears (a) and (b)) is an open gear train submerged in waste water, whereas the epicyclic gear train is a closed gear train located above the surface of waste water. A type series of second-stage open gear trains for scrapers of a diameter from 4 m to 36 m was designed as part of the present project. The details of the analysis and synthesis of second-stage gear train meshing were presented in a study by Batsch et al. (2017). Data used in the design of the planetary gear train were determined on the basis of a dynamic analysis of the entire drive system as well as sedimentation and flotation process requirements.

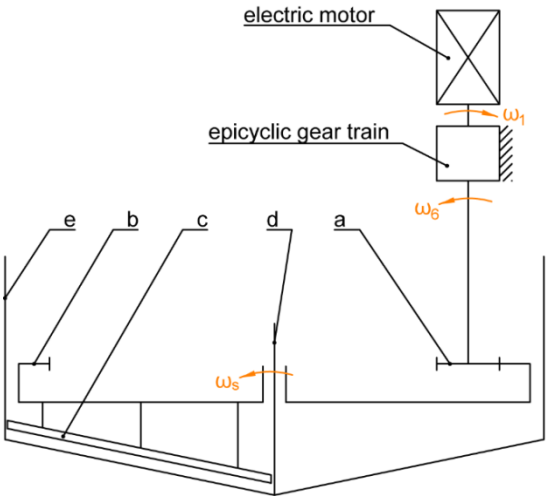

Fig. 1. Proposed kinematic system of a new radial settling tank drive

This paper presents the results of the preliminary calculations of strength of the teeth of a planetary reduction gear designed for radial sedimentation tank drives. Calculations were carried out in accordance with ISO 6336 standard and the finite element meth-

DOI 10.2478/ama-2020-0018

od. The analyses were aimed at selecting the material and determining the condition of the material that would ensure load transmission in the planetary gear train.

2. KINEMATICS

The radial scraper is a device operating at a very low rotation speed (approx. 1 rpm). In order to drive it with a conventional cage induction motor, one should use gearboxes with a large reduction ratio. Planetary gears are one of the gears that allow this while maintaining a relatively small number of reduction stages. There are many design variants of this type of gears, among which a large part has wheels with internal toothing (Dadley, 2002). Finishing this type of teeth can be troublesome due to the need to use special grinding heads. For this reason, it was decided to use the kinematic system of the gears, in which only wheels with external toothing are present. The need to use a large reduction ratio and the desire to use only external gearing prompted the authors to choose gears, whose kinematic diagram is shown in Figure 2.

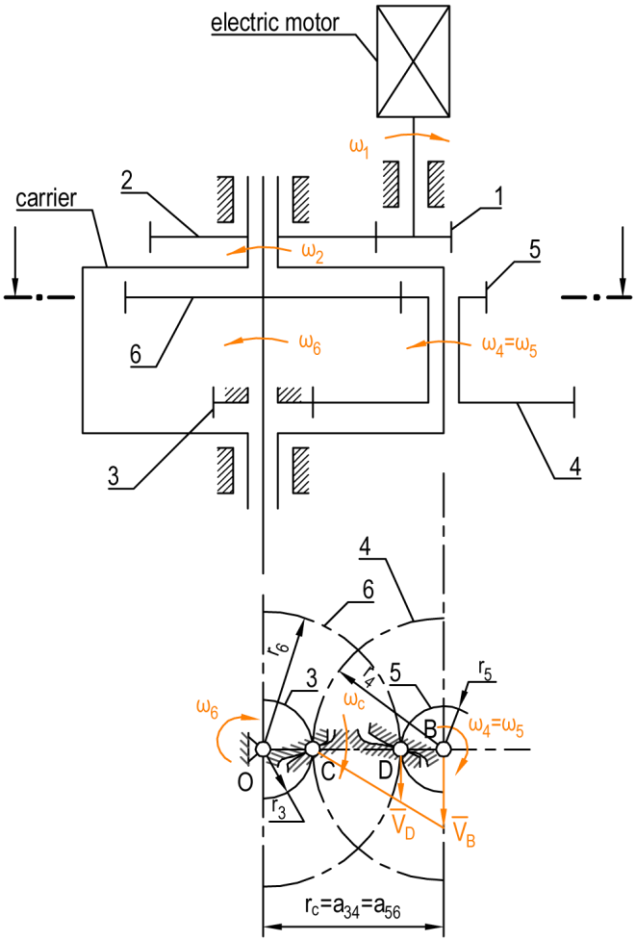

Fig. 1. Kinematic diagram of gear, where: ω_1 – gear 1 angular velocity, ω_2 – gear 2 angular velocity, ω_4 – gear 4 angular velocity, ω_5 – gear 5 angular velocity, ω_6 – gear 6 angular velocity, B – planet's centre of rotation, D – gear 5 & 6 contact point, C – gear 3 and 4 contact point (planet's momentary centre of rotation), O – gear 6 center of rotation, a_{34} – distance between axes of gears 3 and 4, a_{56} – distance between axes of gears 5 and 6

Gear 1, meshing with gear 2, is driven by an electrical motor. Gear 2 has a rigid connection to the carrier. The carrier supports three planets including gears 4 and 5, fixed to each other. Gear 4 rolls against a stationary sun gear (3). Meanwhile, gear 5, meshing with gear 6, transmits velocity and torque to the gear's output shaft. In the discussed case, spur gears were applied, whose parameters are listed in Table 1.

Tab. 1. Gear parameters

Gear no.	Module [mm]	Number of teeth [-]	Profile shift coefficient [-]	Working pitch radius [mm]	Meshing width [mm]
1	2.75	21	0.1799	29.1818	25
2		56	0.2450	77.8182	
3	3	30	0.6110	46.7797	45
4		29	0.7100	45.2203	
5	3.5	26	-0.0786	45.1321	45
6		27	-0.1219	46.8679	

The second gear's (carrier's) angular velocity is given by formula (1):

$$\omega_2 = \omega_c = \omega_1 \frac{r_1}{r_2} \tag{1}$$

where: r_1 – gear 1 rolling radius, r_2 – gear 2 rolling radius. The planet rotates relative to the momentary centre of rotation C. Consequently, from the equality of linear velocities of point B assigned to the carrier and gear 4 stems the following relationship (2):

$$\omega_c = \omega_4 \frac{r_4}{r_c} \tag{2}$$

Likewise, on the basis of the equality of linear velocities of point D assigned to gears 5 and 6, the angular velocity of planet (3) was calculated

$$\omega_4 = \omega_5 = \omega_6 \frac{r_6}{r_4 - r_5} \tag{3}$$

By introducing relationship (3) into formula (2), planetary stage gear ratio (4) was obtained:

$$i_e = \frac{\omega_c}{\omega_6} = \frac{r_4 r_6}{(r_4 - r_5) r_c} = 261 \tag{4}$$

Taking into account cylindrical stage gear ratio $i_c = r_2/r_1$, the overall gear ratio is given by formula (5):

$$i = i_c i_e = \frac{r_2}{r_1} \cdot \frac{r_4 r_6}{(r_4 - r_5) r_c} = 696 \tag{5}$$

3. DISTRIBUTION OF MESHING FORCES

Figure 3 shows the distribution of meshing forces in the planetary gear stage. The carrier is acted upon by torque T_c, resulting from motor torque $T_1 = 1.95Nm$ and the gear ratio of the cylindrical stage (6):

$$T_c = i_c T_1 = 5.20Nm \tag{6}$$

From the equations of the balance of torques acting on the planet, the following relationship (7) may be developed:

$$F_{34} = F_{65} \frac{r_5}{r_4} \tag{7}$$

DOI 10.2478/ama-2020-0018

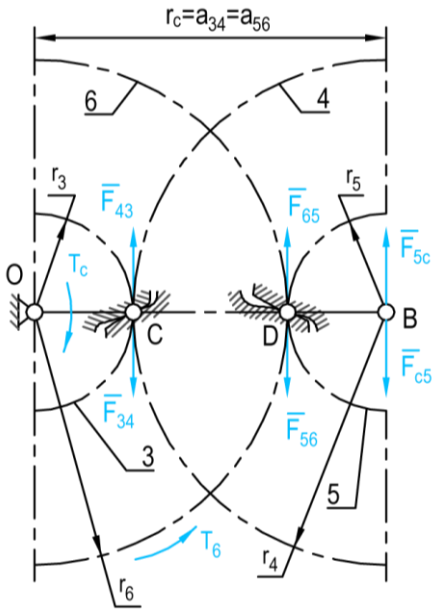

Fig. 3. Distribution of meshing forces in planetary gear stage, where: T_c – carrier torque, F_{34} – circumferential force exerted by gear 3 on gear 4, F_{43} – circumferential force exerted by gear 4 on gear 3, F_{56} – circumferential force exerted by gear 5 on gear 6, F_{65} – circumferential force exerted by gear 6 on gear 5, F_{5c} – circumferential force exerted by planet on carrier, F_{c5} – circumferential force exerted by carrier on planet, T_6 – resistance torque affecting output shaft

By using relationship (7) in the equation, the balance of forces acting on the planet, we may obtain (8):

$$F_{c5} = F_{65}\frac{r_4 - r_5}{r_4} \tag{8}$$

Taking into account that $F_{c5} = \frac{T_c}{r_c}$, the circumferential force at point D is given by formula (9):

$$F_{65} = \frac{T_c}{r_c}\frac{r_4}{r_4 - r_5} = 29006N \tag{9}$$

By introducing relationship (9) into (8), we ultimately arrive at the circumferential force at point C (10):

$$F_{34} = \frac{T_c}{r_c}\frac{r_5}{r_4 - r_5} = 28949N \tag{10}$$

The above equations were derived for a case in which a single planet gear occurs. In reality, in meshing force calculations, one must include the number of planet gears n and the load distribution coefficient K_γ according to formulas (11):

$$F'_{34} = \frac{K_\gamma}{n}F_{34};\ F'_{65} = \frac{K_\gamma}{n}F_{65} \tag{11}$$

In a perfect situation (even load distribution over planet gears $K_\gamma = 1$) all forces balance out, exerting no stress on the bearings of the output shaft or the carrier. The bearings may be stressed if the distribution of the load becomes uneven, and the forces do not balance out entirely.

4. STRENGTH ASSESSMENT ACCORDING TO ISO 6336

Strength calculations were limited to determining nominal stress values resulting from static tooth load.

4.1. Contact stress

Following the ISO 6336-2 (2006) standard, nominal contact stress values are given by formula (12):

$$\sigma_{H0} = Z_H Z_E Z_\varepsilon \sqrt{\frac{F'}{db}\cdot\frac{u+1}{u}} \tag{12}$$

where: Z_H – zone factor, Z_E – elasticity factor, Z_ε – contact ratio factor, F' – circumferential force, d – drive gear pitch diameter, b – ring width, u – gear pair ratio. Calculation procedures determining individual coefficients were described in the above-mentioned standard. The resulting stress values for individual gear pairs are shown in Table 2.

Tab. 2. Analytically-determined contact stress values

	Mesh load factor K_γ [-]				
	0.7	1	1.1	1.2	1.3
	Nominal contact stress σ_{H0} [MPa]				
Gear pair 1-2	103.20				
Gear pair 3-4	712.01	851.02	892.56	932.25	970.31
Gear pair 5-6	776.04	927.54	972.81	1016.07	1057.56

4.2. Root stress

As it is given in ISO 6336-3 (2006) standard, nominal root stress values are calculated by means of formula (13):

$$\sigma_{F0} = Y_F Y_S \frac{F'}{bm} \tag{13}$$

where: Y_F – form factor, Y_S – stress correction factor, F' – circumferential force, m – module, b – meshing width. Calculation procedures for determining individual coefficients were described in the above-mentioned standard. The resulting stress values for individual gears are shown in Table 3.

Tab. 3. Analytically-determined root stress

	Mesh load factor K_γ [-]				
	0.7	1	1.1	1.2	1.3
	Nominal root stress σ_{F0} [MPa]				
Gear 1	2.79				
Gear 2	2.80				
Gear 3	148.40	212.00	233.20	254.40	275.60
Gear 4	146.02	208.61	229.47	250.33	271.19
Gear 5	118.60	169.43	186.37	203.32	220.26
Gear 6	119.89	171.27	188.40	205.53	222.65

5. FEM SIMULATION

5.1. Computational model

Numerical calculations of the gear motor were performed in Abaqus software by means of the finite element method (FEM). Key stress values were determined based on the models that accurately represent the dimensions of real gearbox components. These were compared with results obtained from analytical calcu-

lations. To simplify finite element model, the entire task was split into three phases, which covered consecutive gear motor stages.

Since the gearing contains cylindrical spur gears, numerical FEM calculations were performed using flat models based on the plane stress states theory developed by Rusiński et al. (2000). For each of the stages, computational models were cross-sections through the center of the width of gears of a particular gearing stage. Such procedure, as it was concluded by Kopecki and Witek (2000) and by Rusiński et al. (2000), guarantees accurate results with considerably shorter calculation and result processing time.

It was assumed that the gears are made of steel of the following parameters: Young's modulus $2.05 \cdot 10^{11}$ Pa, Poisson coefficient 0.3. All boundary conditions, loads, restraints and displacements were defined according to the analytically pre-calculated values and the adopted kinematic system. Frictionless contact between the carrier and the planet gear (item 3 in Fig. 4) was assumed. The axis of the carrier was connected with a rigid body to the axis of the sun gear (item 4 in Fig. 4). In this case, the effect of play on the planet gears or errors in the geometry in the actual gear train were not investigated. The carrier axis was allowed to moved only over a circle, the center of which was placed on the axis of the sun gear. The movement of the carrier arising from the gear train kinematics was forced, and resistance (torque) was defined on the planetary gear due to its connection to gear 5 (Fig. 2).

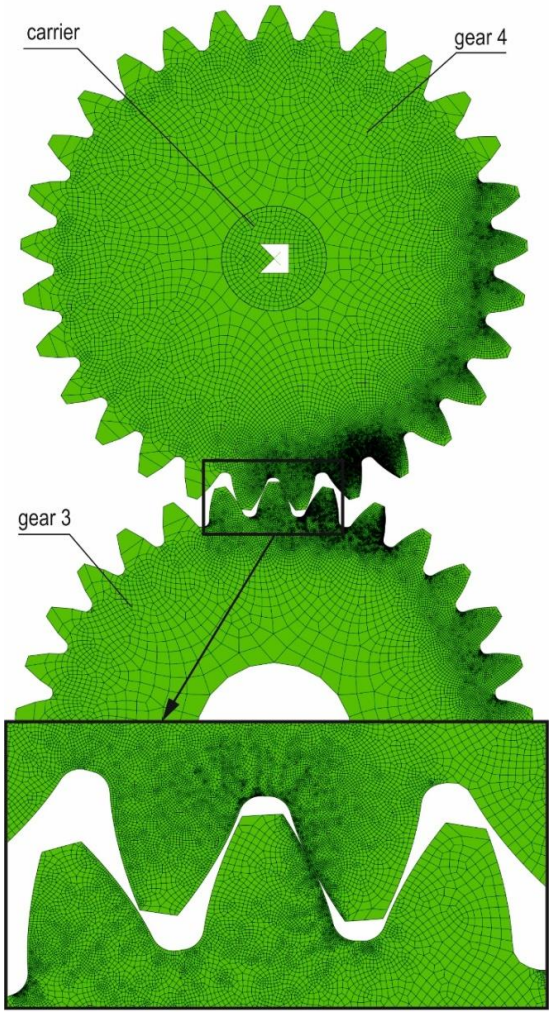

Fig. 4. Gear model designed for calculations in Abaqus software

The models were discretized, that is, divided into finite elements in an uneven manner according to the recommendations formulated by Budzik and Pacana (2008) and Kopecki and Witek (2000). Definitely, the largest density of nodes was present in the toothed ring area, with lower density in other locations on the models, which can be seen in Figure 4. Also, within a single tooth, differentiation of the mesh was introduced by using several times more finite elements in the discretization of the active tooth flank than for its passive side (Fig. 4). It made possible to shorten the calculations and to get highly accurate results in key areas. The discretization performed in Abaqus's pre-processor, CPS4R quadrilaterals were used.

Figure 4 presents an overview of the model prepared for calculations in Abaqus software for the second gear stage. Apart from gears 3 and 4, a model of the carrier was also included, through which rolling trajectory for the planet gear was defined. Grid density in the area of the toothed rings of engaging gear models is clearly visible.

In the process of the analysis, both the model preparation and computational methods were kept the same for three stages of the gear.

5.2. Calculation results

The basic form in which the results were obtained was the distribution of reduced stress presented on previously prepared models. The analysis focused on the gear meshing area, where the highest stress values were recorded. The area is of fundamental importance in terms of strength. Figure 5 shows sample results for the second stage of the gearbox.

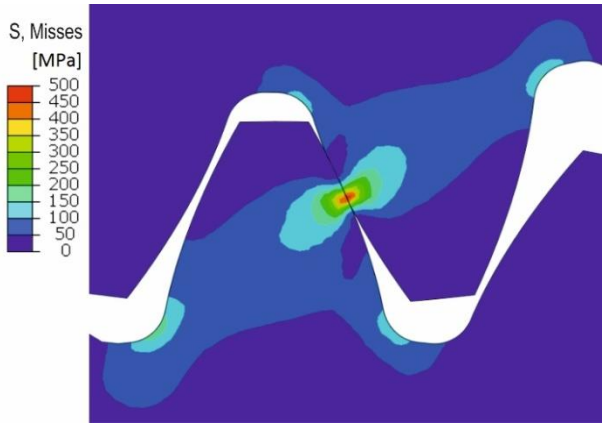

Fig. 5. Distribution of reduced stress in gear 3 and 4 meshing area

Evidently, the highest stress values were recorded at the point of contact between the flanks of meshing teeth. Stress concentration is also present at the opposite side of the teeth. In accordance with ISO 6336-1 (2006) standard, stress in these areas constitutes a basic criterion for assessing the correctness of the designed gear. The results showed as stress distribution and helped to identify areas at risk. However, they are insufficient to perform precise strength calculations. In order to increase clarity, the results may be presented as charts. Figures 6 and 7 show sample reduced root stress values for gears 3 and 4. The illustrations also contain schematic charts taken into account in analytical calculations according to a generally approved literature on

strength calculations and gear performance quality (Sánchez et al., 2019). Here, we assume a rectilinear load distribution, evenly divided into three stages of engagement. As can be seen, the real nature of load exerted on a gear tooth is slightly different. It does not interfere with general-purpose gear calculations, however, when designing more demanding systems, one must take into account more accurate results offered by the numerical FEM method.

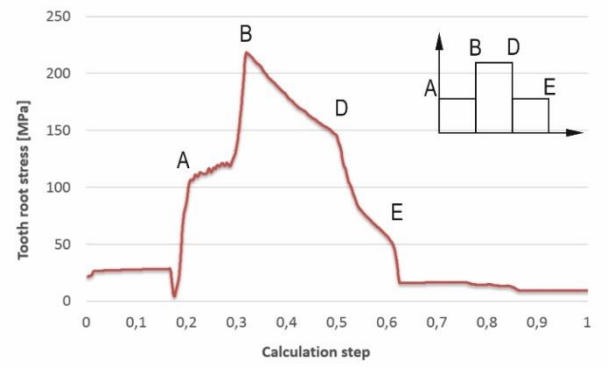

Fig. 6. Changes in reduced root stress values in gear 3 (A, B, D, E – characteristic points on path of contact, A – entry into engagement of second tooth (two-pair meshing), B – lowest point of single tooth contact (LPSTC), D – highest point of single tooth contact (HPSTC), E – exit from meshing of second tooth)

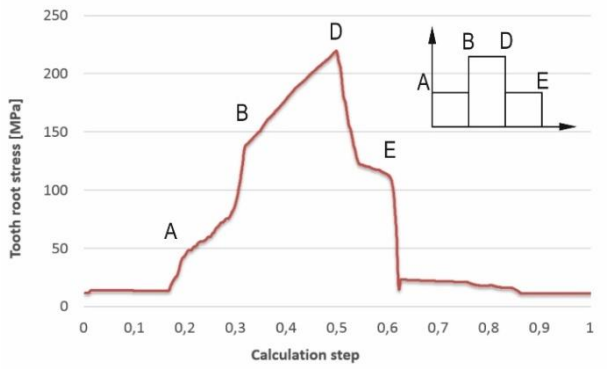

Fig. 7. Changes in values of reduced root stress in gear 4 (A, B, D, E – characteristic points on path of contact, description as in Fig. 5)

Charts illustrating reduced root stress as well as contact stress values for all gears of the analyzed gearing were created on a similar basis. This helped trace the moments where extreme values occurred and read their quantity. Subsequently, one may compare the results obtained in numerical calculations with the ones generated in analytical calculations and confirm their mutual consistency.

5.3. Uneven load distribution

As multipath gears are characterized by the risk of uneven load distribution on each of the paths (Parker and Lin, 2004; Budzik et al. 2013), the issue was also examined in the analysis.

In the initial solution for $K_\gamma = 1$, each of the three planets carried the same load. Knowing that during its operation, the torque value transmitted by each path is variable, such assumption was also made in FEM numerical calculations. It was assumed that the maximum practically foreseeable value of the mesh load factor would occur (ANSI/AGMA 6123-C16), and the load at the second and third stage of the gear motor was proportionally increased. An inverse situation was also taken into account, with the planet transmitting a torque lower than nominal, because the two remaining ones carry a higher load. The results of numerical calculations obtained for the initial case and for inequality coefficients of 0.7, 1.1, 1.2 and 1.3 were juxtaposed to compare how unbalanced load distribution affects stress values in the gears of a planetary gearing.

The results for reduced root stress and contact stress for all wheels of speed reducing gears were listed in Tables 4 and 5.

Tab. 4. Contact stress values on basis of numerical FEM calculations

	Mesh load factor K_γ [-]				
	0,7	1,0	1,1	1,2	1,3
	Contact stress [MPa]				
Gear pair 1-2	112,21				
Gear pair 3-4	698,98	898,45	914,51	938,44	978,98
Gear pair 5-6	813,42	937,44	966,54	997,12	1012,81

Tab. 5. Reduced root stress on basis of numerical FEM calculations

	Mesh load factor K_γ [-]				
	0,7	1,0	1,1	1,2	1,3
	Tooth root stress [MPa]				
Gear 1	2,71				
Gear 2	2,67				
Gear 3	157,96	222,74	242,49	263,28	284,73
Gear 4	156,32	224,80	245,00	266,69	288,67
Gear 5	117,55	183,21	190,35	198,53	206,42
Gear 6	126,61	189,14	197,46	205,35	212,25

6. COMPARISON OF RESULTS

The results are presented in charts (Figures 8 and 9).

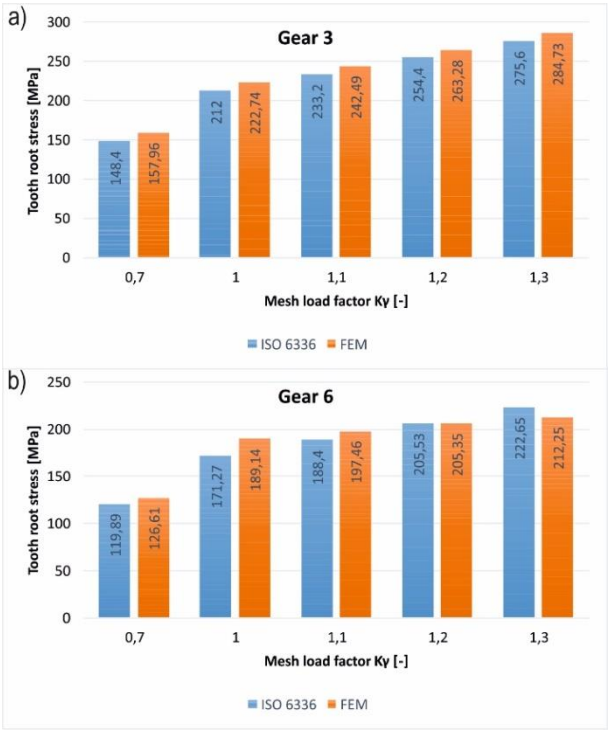

Fig. 8. Reduced root stress for: a) gear 3, b) gear 6

Reduced root stress values determined by FEM simulation approximate those obtained analytically. FEM error with respect to the analytical method reaches a maximum of 10.43% with a reduced stress difference of 17.87 MPa for gear 6 and mesh load factor 1.0. In addition, the largest differences in reduced root stress occur for all wheels with a load distribution coefficient equaling 1.0.

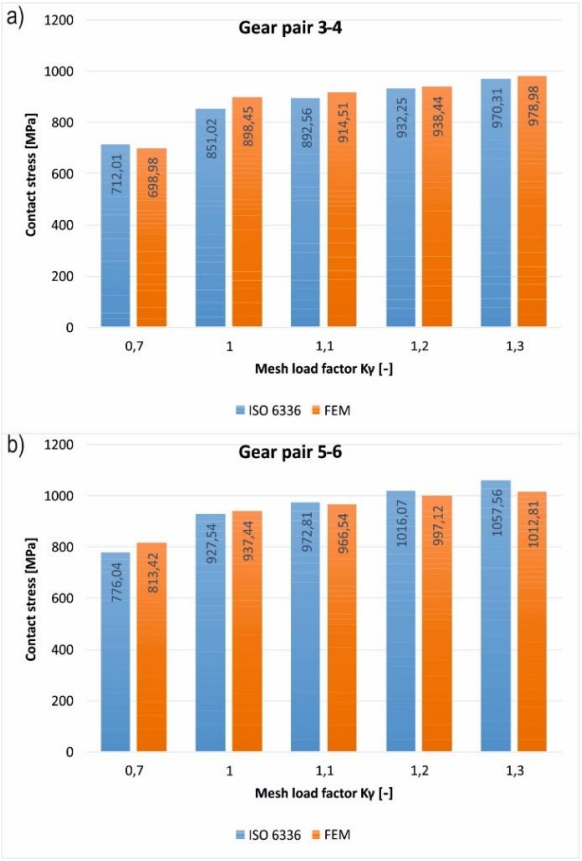

Fig. 9. Contact stress values for: a) pair 3-4, b) pair 5-6

In the case of contact stress, it was noted that the FEM error related to the analytical method shows neither an upward nor a downward trend with increasing load (increase of load distribution coefficient). The largest difference in the value of reduced stress 47.43 MPa, constituting approx. 5.6% of the value of analytical stress occurred for the mash load factor 1.0 (Fig. 9b).

7. SUMMARY AND CONCLUSIONS

On the basis of the performed calculations and simulations, it can be concluded that:

- The first gearing stage is slightly loaded, and gears 1 and 2 can be made of quenched and tempered steel, for example, 42CrMo4.
- The epicyclical stage of the gearing is subjected to the highest load, and bending and contact stresses necessitate the use of steel for surface hardening (nitriding or carburizing and hardening).

In addition, the mesh load factor over planets has a significant effect on the selection of the material for planetary stage gears (gear pairs 3-4 and 5-6). It depends in particular on how the planet and sun gears are mounted, the positioning accuracy on the carrier, tooth fabrication accuracy and, in the planetary gearing discussed in this study, the accuracy of the positioning of the teeth of gear 5 relative to gear 4. Guidelines contained in ANSI/AGMA 6123-C16 (2016) standard, as well as simulations and calculations performed prompted the authors to form the following conclusions:

- If planet and sun gears are supported without flexible mounts, and gears are made to class 7 (mesh load factor according to ANSI/AGMA 6123-C16 (2016) standard equals 1.23), gears should be made of carbon steel for carburizing and hardening.
- If planets are flexibly mounted or flexible clutches are used and gears are made to class 4 (mesh load factor according to ANSI/AGMA 6123-C16 (2016) standard equals 1), gears may be made of steel for nitriding.

The analysis of the load capacity of a multi-path gearing presented in this study was aimed to determine the locations of potential failures and work-flow hazards. Apart from gear contact areas, no other locations of increased stress values were found. One should note, however, that stress values obtained in numerical calculations are slightly different from the actual ones. This is due to both the use of discrete models as well as a simplified load pattern. Numerical analyses did not include, for example, friction, safety or overload factors. Without these additional parameters, the stresses calculated by numerical FEM often do not yield ultimate results. The obtained results allow to identify risks or simulate engagement, providing very useful information for design purposes. However, they should always be checked by means of other computational or experimental methods. Verification of the results enables the introduction of suitable similarity coefficients into numerical calculations. This makes them an even more useful tool in the hands of a gear engineer.

REFERENCES

1. **ANSI/AGMA 6123-C16** (2016), Design Manual for Enclosed Epicyclic Gear Drives.
2. **Batsch M., Markowski T., Zubrzycki M.** (2017), Mathematical model of internal pin gear mesh (in Polish), *STAL Metale Nowe technologie.* Koła zębate - projektowanie, wytwarzanie, pomiary, eksploatacja, 13–16.
3. **Budzik G., Kozik B., Pacana J.** (2013), Defining influence of load conditions on distribution and value of stresses in dual-power-path gear wheels applying FEM, *Aircraft Engineering and Aerospace Technology*, Vol. 85, No. 6, 453–459.
4. **Budzik G., Pacana J.** (2008), Analysis of the correctness of the FEM solution depending on the type and number of finite elements used (in Polish), *Acta Mechanica Slovaca*, 3-A/2008, t. 12, Technical University of Kosice, 327–332.
5. **Cooley C.G., Parker R.G.** (2014) A review of planetary and epicyclic gear dynamics and vibrations research, *Applied Mechanics Reviews*, Vol. 66, No. 4, Article Number 040804
6. **Dadley D.W.** (2002), *Handbook of Practical Gear Design*, CRC Press LLC.
7. **Fernandez del Rincon A., Viadero F., Iglesias M., García P., de-Juan A., Sancibrian R**. (2013) A model for the study of meshing stiffness in spur gear transmissions, *Mechanism and Machine Theory*, Vol. 61, 30–58, doi.org/10.1016/j.mechmachtheory.2012.10.008
8. **Iglesias M., Fernandez del Rincon A., de-Juan A., Garcia P., Diez-Ibarbia A., Viadero F.** (2017) Planetary transmission load sharing: Manufacturing errors and system configuration study, *Mechanism and Machine Theory*, Vol. 111, 21–38, https://doi.org/10.1016/j.mechmachtheory.2016.12.010.

9. **ISO 6336-1** (2006), Calculation of load capacity of spur and helical gears — Part 1: Basic principles, introduction and general influence factors.
10. **ISO 6336-2** (2006), Calculation of load capacity of spur and helical gears — Part 2: Calculation of surface durability (pitting).
11. **ISO 6336-3** (2006), Calculation of load capacity of spur and helical gears — Part 3: Calculation of tooth bending strength.
12. **Kopecki H., Witek L.** (2000), Influence of the type and number of elements on the error and convergence of the FEM solution on the example of the stability analysis of a compressed member (in Polish). *V Konferencja Naukowo-Techniczna, Military University of Technology*, *(WAT)*, IPPT PAN, Warsaw - Rynia.
13. **Ligata H., Kahraman A., Singh A.** (2008), An experimental study of the influence of manufacturing errors on the planetary gear stresses and planet load sharing, *Journal of Mechanical Design*, Transactions of the ASME, Vol. 130, No. 4, 577–595.
14. **Markowski T., Budzik G., Pacana J.** (2010), Criteria for selecting a numerical model for the strength calculations of a cylindrical gear with the FEM method (in Polish), *Modelowanie Inżynierskie*, Vol. 8, No. 39, 135–142.
15. **Marques P.M.T., Martins R.C., Seabra, J.H.O.** (2016) Power loss and load distribution models including frictional effects for spur and helical gears, *Mechanism and Machine Theory*, Vol. 96, Part 1, 1–25, DOI: 10.1016/j.mechmachtheory.2015.09.005
16. **Marques P.M.T., Martins R.C., Seabra, J.H.O.** (2017) Analytical load sharing and mesh stiffness model for spur/helical and internal/external gears – Towards constant mesh stiffness gear design, *Mechanism and Machine Theory,* Vol. 113, 126–140, doi.org/10.1016/j.mechmachtheory.2017.03.007
17. **Parker R.G., Lin J.** (2004) Mesh Phasing Relationships in Planetary and Epicyclic Gears, *Journal of Mechanical Design, Vol. 126(2), 365–370, https://doi.org/10.1115/1.1667892*
18. **Rusiński E., Czmochowski J., Smolnicki T.** (2000), *Advanced finite element method in load-bearing structures* (in Polish), The Wrocław University of Technology Publishing House, Wrocław.
19. **Sánchez M.B., Pleguezuelos M., Pedrero J. I.** (2019), Strength model for bending and pitting calculations of internal spur gears, *Mechanism and Machine Theory*, Vol. 133, 691–705, https://doi.org/10.1016/j.mechmachtheory.2018.12.016
20. **Singh A.** (2005), Application of a System Level Model to Study the Planetary Load Sharing Behavior, *Journal of Mechanical Design*, Vol. 127, 469–476.
21. **Singh A.** (2010), Load sharing behavior in epicyclic gears: Physical explanation and generalized formulation, *Mechanism and Machine Theory*, Vol. 45, 511–530.
22. **Tsai S.-J., Huang G.-L., Ye S.-Y.** (2015) Gear meshing analysis of planetary gear sets with a floating sun gear, *Mechanism and Machine Theory*, Vol. 84, 145–163, https://doi.org/10.1016/j.mechmachtheory.2014.03.001
23. **Tsai S.-J., Ye S.-Y.** (2018), A computerized approach for loaded tooth contact analysis of planetary gear drives considering relevant deformations, Mechanism and Machine Theory, Vol. 122, 252–278, https://doi.org/10.1016/j.mechmachtheory.2017.12.026
24. **Wiktor J.** (2004), *Analytical and numerical methods of analysis of geometric parameters, motion disturbances and strength of cylindrical gears* (in Polish), The Rzeszów University of Technology Publishing House, Rzeszów.

Studies carried out as part of project “Designing an innovative type of a scraper with an integrated planetary drive for new or modernized sedimentation tanks,” No. POIR.01.01.01-00-0286/15-00 under Action 1.1 “R&D Projects of Businesses,” Sub-Action 1.1.1 “Industrial research and development work performed by businesses” POIR in 2015. Competition 1/1.1.1/2015 of the Intelligent Development Operation Programme 2014–2020 co-funded from the European Regional Development Fund.